

## Lateral *n-i-p-i* superlattices in Si metal-oxide-semiconductor structures

A. Huber, H. Lorenz, and J. P. Kotthaus

*Sektion Physik, Universität München, D-80539 München, Germany*

S. Bakker and T. M. Klapwijk

*University of Groningen, Department of Applied Physics, Nijenborgh 4, NL-9747 AG Groningen, The Netherlands*

(Received 29 August 1994)

A stacked-gate technique is used to realize a large lateral potential modulation in microstructured silicon metal-oxide-semiconductor samples, thus making possible the search for closely spaced alternating quasi-one-dimensional channels of electrons and holes. Far-infrared transmission spectra measured at liquid-helium temperature show, besides the well-known absorption in electron quantum wires, an additional signal due to one-dimensional hole channels. With appropriate gate voltages applied to the top and bottom gate the transition from a two-dimensional hole system and a two-dimensional electron system to a so-called lateral *n-i-p-i* superlattice is investigated in magnetic fields up to 15 T.

### I. INTRODUCTION

In the past two decades miniaturization of semiconductor structures has been a provoking task both in basic research and applied physics. Many investigations have been devoted to low-dimensional electron systems in silicon metal-oxide-semiconductor (MOS) samples. The interest is motivated in part by possible implementation of these structures in highly integrated circuits.

Submicrometer lithography renders the fabrication of a periodic sequence of metal stripes as the gate electrode. Thereby the electrons can electrostatically be confined to a one-dimensional electron system (1DES).<sup>1</sup> In a stacked-gate geometry an additional dielectric layer electrically isolates the microstructured bottom gate from the homogeneous top gate (Fig. 1). The two gates enable us to control the electron density and the lateral potential modulation almost independently from each other. The transport<sup>1-3</sup> and far-infrared<sup>4,5</sup> (FIR) properties of the electrons in such specially designed Si MOS samples have been studied intensively in recent years. Furthermore, in

MOS structures with a homogeneous gate the band bending at the semiconductor-isolator interface achieves about 1 eV relative to the substrate by switching over from the flatband case to an inversion layer by using appropriate gate voltages.

We report on FIR transmission studies of Si stacked-gate samples with lateral potential modulations exceeding the fundamental energy gap in Si ( $E_g \approx 1.17$  eV for  $T = 2$  K). These devices make it possible to induce hole channels at the Si-SiO<sub>2</sub> interface below the metallic stripes of the bottom gate and in between electrons below the homogeneous top gate, or vice versa. We call this arrangement of alternating electron and hole quantum wires (Fig. 1) a lateral *n-i-p-i* superlattice, in analogy to vertically grown *n*- and *p*-doped layers.<sup>6</sup> In these doping superlattices, predominantly investigated in the GaAs material system, the electronic and optical properties, e.g., the effective energy gap, can be tuned in a large range. Beyond that, theory<sup>7</sup> predicts an interesting behavior of the plasma excitations in these type-II superlattices. In the weak-coupling limit between adjacent layers, the well-known electron and hole plasmons of a quasi-two-dimensional system exist. In the strong-coupling regime acoustic and optical plasma modes arise, similar to the phonon dispersion in solid-state physics. Here in our stacked-gate samples the transition from a two-dimensional electron (2DES) or hole system (2DHS) to a lateral *n-i-p-i* structure can be studied. Instead of doping, electrostatics on essentially undoped substrates is used to establish and tune the lateral *n-i-p-i* superlattice. At moderate potential modulations we observe dimensional resonances of holes (*h*-DR) and electrons (*e*-DR) in one-dimensional channels. In a two-dimensional system, in contrast to Si bulk material, the effective mass of the electrons and holes is strongly dependent on the carrier density.<sup>8,9</sup> At very low hole densities and high magnetic fields the *h*-DR is found to show a pronounced peak structure, whereas at high hole densities we observe a Drude-like absorption.

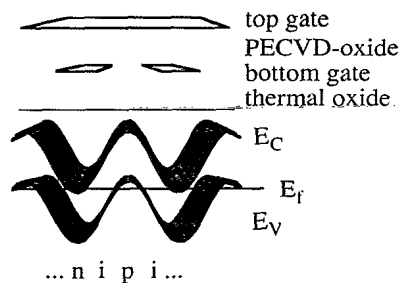


FIG. 1. Schematic side view of a stacked-gate sample. The lateral modulation of the conduction- ( $E_c$ ) and valence-band ( $E_v$ ) edges at the Si-SiO<sub>2</sub> interface is indicated. If the Fermi energy  $E_f$  intersects both band edges in equilibrium, adjacent electron (*n*) and hole layers (*p*) separated by intrinsic layers (*i*) form a lateral *n-i-p-i* superlattice.

## II. EXPERIMENTAL DETAILS

For the sample fabrication we use thermally oxidized *p*-type (100)-Si wafers with an oxide thickness of 40 nm (32 nm) for sample A (B) and a preferential low substrate doping concentration  $N_{\text{Bor}} \approx 1 \times 10^{14} \text{ cm}^{-3}$ . Via holographic lithography and lift-off technique, a periodic metal grating is defined. The period  $a$  of the gate is 500 nm (300 nm) for sample A (B). The linewidth  $w$  of a single metal stripe is 320 (sample A) and 200 nm (sample B). A second oxide layer is formed by a plasma-enhanced chemical-vapor deposition (PECVD) process in order to isolate the homogeneous top gate from the bottom gate. This PECVD oxide is 75 nm thick for sample A and 139 nm for sample B, respectively (Fig. 1). The homogeneity of the bottom gate stripes is controlled by a scanning electron microscope and capacitance measurements.

The experiments are performed in a FIR Fourier-transform spectrometer at  $T=2 \text{ K}$  and magnetic fields up to 15 T, oriented perpendicular to the sample surface. The FIR radiation is guided by a brass pipe from the Michelson interferometer onto the sample and the transmitted intensity is detected by a Si bolometer. To generate inversion electrons in *p*-type Si and to establish quasiequilibrium between the Fermi energies of the back contact and the inversion electrons under bias at low temperatures, it is necessary to illuminate the sample shortly before recording the absorption spectrum with above-band-gap light. To induce an accumulation layer at the interface, thermal room-temperature background radiation is sufficient.

In the present case of small signal variation and stripe geometry, the following expression<sup>10</sup> for the transmission  $T$  is a good approximation:

$$-\frac{\Delta T}{T} = 1 - \frac{T(N_L)}{T(0)} \propto \text{Re}(\sigma(N_L, \omega)). \quad (1)$$

The last term of (1) represents the real part of an effective dynamic conductivity. Due to the large wavelength ( $\lambda \gg a$ ), the FIR radiation averages over several electron stripes. Therefore  $N_s$  in the conductivity of a 2DES can be replaced by the line density  $N_L = N_s a$ .

## III. LATERAL *n-i-p-i* SUPERLATTICES

The FIR excitations in quasi-two- and quasi-one-dimensional electron and hole systems have been investigated in two stacked-gate structures with slightly differing sample parameters. The electron and hole systems are electrostatically defined by the two gate electrodes. Therefore it is feasible to tune between different states, for example from a 1DES to a lateral *n-i-p-i* superlattice.

Figure 2 shows FIR spectra of sample A taken at a fixed top-gate voltage  $V_{\text{tg}} = 7 \text{ V}$  and different bottom-gate voltages  $V_{\text{bg}}$ . In this configuration and for  $B = 0 \text{ T}$  the threshold voltage  $V_{T,e}$  for forming inversion electrons under the lower gate is  $-0.5 \text{ V}$ . For bottom-gate voltages slightly higher than  $V_{T,e}$ , two resonances are observed. Their energy can be associated with plasmons in a 2DES and a wave vector  $k$  given by  $n(2\pi/a)$  ( $n = 1, 2, \dots$ ).

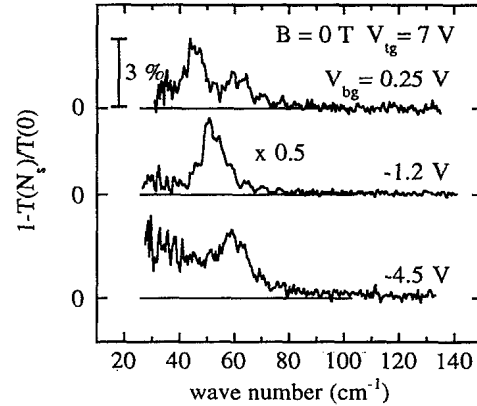


FIG. 2. Plasmon excitations in a density-modulated 2DES ( $V_{\text{bg}} = 0.25 \text{ V}$ ) and electron dimensional resonances ( $V_{\text{bg}} = -1.2 \text{ V}$  and  $V_{\text{bg}} = -4.5 \text{ V}$ ) in a 1DES in Si between the metal stripes of the bottom gate (sample A) at  $B = 0 \text{ T}$  and  $T = 2 \text{ K}$ . For  $V_{\text{bg}} = -4.5 \text{ V}$  besides the *e*-DR a Drude-like absorption by holes is observed in addition to the *e*-DR.

Both the metal grating and the density modulation of the 2DES enable coupling of FIR radiation to quasi-two-dimensional plasmon excitations with wave vectors  $k = 2\pi/a$  and  $k = 2(2\pi/a)$  determined by the lateral periodicity  $a$  of the structure. The dipole excitation of the plasmon with  $n = 2$  is allowed in this nonsymmetric gate geometry, because the width of a single gate finger is larger than the gap opening.

For  $V_{\text{bg}} = -1.2 \text{ V} < V_{T,e}$  isolated inversion channels are formed, and the electrons are confined in quantum wires in Si between the stripes of the bottom gate (gap confinement mode for electrons). The dominant far-infrared excitation of such an electron system is called a depolarization or a dimensional resonance. With further decreasing bottom-gate voltage, an additional broad absorption signal appears at low frequencies and is interpreted as resulting from the dynamic conductivity of holes below the bottom gate (subgrating mode for holes). In this case we have realized an alternating series of electron and hole quantum wires, a so-called lateral *n-i-p-i* structure. The effective hole mass<sup>9</sup> of about  $m^* \approx 0.5m$  for  $N_s = 2 \times 10^{12} \text{ cm}^{-2}$ , and the low mobility of holes result in a Drude-like absorption  $\sigma(\omega) \sim 1/(1 - i\omega\tau)$  with the relaxation time  $\tau$ . The formation of a hole channel is accompanied by the shift of the *e*-DR to higher energies. With a lowering of the bottom-gate voltage the curvature of the lateral potential and hence the confinement energy is increased. Note that the oscillator strength as estimated from the change in transmission is diminished for  $V_{\text{bg}} = -4.5 \text{ V}$  compared to  $V_{\text{bg}} = -1.2 \text{ V}$ . This fact demonstrates that in the gap confinement mode for electrons the effective electron density is not fixed by the top gate, but rather that the electron stripes can be squeezed with  $N_s$  lowered by the bottom gate.

The dependence of the electron resonance positions at fixed  $V_{\text{tg}}$  on  $V_{\text{bg}}$  is shown in Fig. 3. Starting at positive bottom-gate voltages the energy of the plasmons in a density-modulated 2DES decreases. As already shown in previous experiments,<sup>11</sup> this is dominantly due to the fact

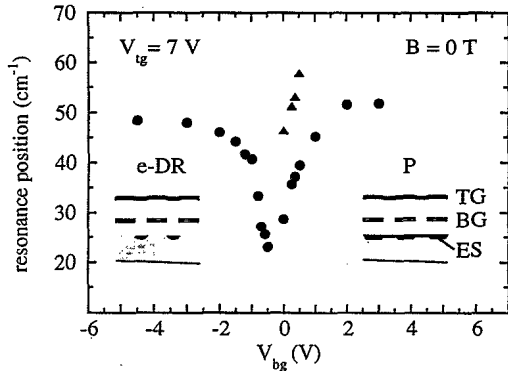


FIG. 3. Transition from a density-modulated 2DES ( $P$  indicates plasmons) to isolated electron channels ( $e$ -DR) in the gap confinement mode for  $B = 0$  T (sample A). The triangles mark higher plasmon modes. The insets show the cross section of a stacked-gate sample with the top (TG) and bottom (BG) gates, and the corresponding electron system (ES) in the different bottom gate voltage regimes.

that the average electron density declines. In a small voltage interval of about 0.5 V in addition to the fundamental plasmon at  $k = 2\pi/a$ , the next-higher plasmon mode ( $k = 4\pi/a$ ) is observed. In this voltage regime close to the threshold for electrons, the strong density modulation acts as an active grating coupler to induce higher plasma excitations. The ratio for the plasmon energies  $\omega_p(n=2)/\omega_p(n=1)$  yields an average value of 1.38, in good agreement with the theoretical prediction of  $\sqrt{2}$ . For  $V_{bg} < V_{T,e}$ , only one single  $e$ -DR is observed. This fact reflects that the bare potential shape for electrons in the gap confinement mode has an almost parabolic shape, and that therefore only the Kohn mode<sup>12,13</sup> can be excited. However, in the subgrating mode for electrons we observe higher orders of the  $e$ -DR (in analogy to  $n = 3$  and 5 in Ref. 4) for large voltage differences between the two gates, and revealing nonparabolic portions in the bare potential, but with low oscillator strength. This demonstrates that even in small grating finger structures nonparabolicity of the bare potential is achievable, but plays a subordinate role.

FIR spectra of the transition from a 1DES to a lateral  $n$ - $i$ - $p$ - $i$  superlattice are displayed in Fig. 4. Opposite to Fig. 2, now the electrons are induced in the subgrating mode. With decreasing top-gate voltage, holes are accumulated between the opening of the lower gate. The threshold voltage for electrons in this arrangement was found to be about  $-1.5$  V. Decreasing the top-gate voltage from  $V_{tg} = -2$  V to  $V_{tg} = -9$  V, the energy of the  $e$ -DR strongly shifts to higher values and saturates at low  $V_{tg}$  at  $39$   $\text{cm}^{-1}$ . Assuming a parabolic potential shape  $V_0 = (1/2e)m^* \omega_0^2 (a/4)^2$  for a half-period of the superlattice potential with a potential modulation of  $2V_0 \approx$  energy gap/ $e = 1.17$  V, a resonance frequency of  $\omega_0 = 43$   $\text{cm}^{-1}$  is calculated for  $m^* = 0.2m$  and a period  $a$  of 500 nm. The result of this simplified model is in good agreement with the experiment. More refined numerical electrostatic calculations neglecting charge accumulation at the insulator-semiconductor interface showed that indeed

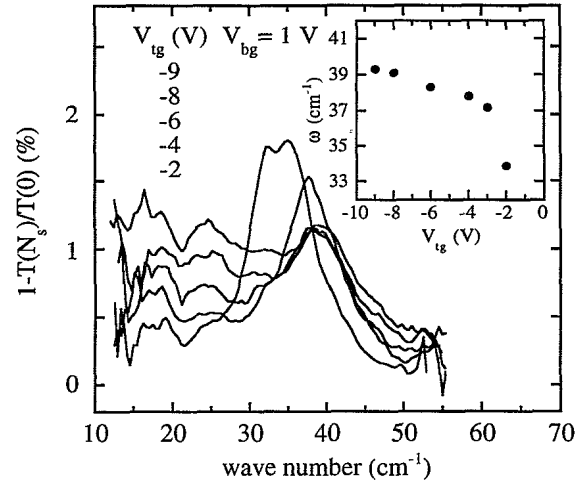


FIG. 4. Transition from electron quantum wires to a lateral  $n$ - $i$ - $p$ - $i$  superlattice. The increasing absorption signal dominantly at low wave numbers is caused by the absorption of holes (sample A). The inset shows the energy position of the  $e$ -DR.

at  $V_{bg} = 1$  V and  $V_{tg} = -9$  V a potential modulation of about 1.5 V at the Si-SiO<sub>2</sub> interface is achieved. In these simulations Laplace's equation was solved for a mesh of  $82 \times 100$  data points representing the geometrical cross section of sample A. Appropriate boundary conditions were used, and screening effects of the mobile carriers neglected.

In the following, experimental results for sample B at high magnetic fields are discussed. These fields shift the resonance energy of the excitations at  $B = 0$  T to a higher-frequency regime, where (e.g.) hole resonances may be better resolved by the Fourier spectrometer. There threshold voltage for holes in the subgrating mode at a magnetic field of  $B = 13$  T is found to be  $V_{T,h} = -1$  V. For  $V_{tg} = -4$  V and  $V_{bg} = -2$  V, and almost homogeneous two-dimensional hole system (2DHS) is induced at the interface showing the typical Drude-like behavior (Fig. 5). For gate voltages close to the threshold voltage for holes, there is a pronounced resonance at  $35$   $\text{cm}^{-1}$  which we identify as dimensional resonance ( $h$ -DR) in a quasi-one-dimensional hole channel. Increasing  $V_{tg}$  to above the threshold voltage for electrons  $V_T = -0.6$  V, in addition inversion electrons in narrow quantum wires are generated and an additional resonance appears at about  $70$   $\text{cm}^{-1}$ , which we identify as the dimensional resonance of electrons in narrow quantum wires in between the hole channels.

To substantiate the above identification, we introduce an additional experiment as illustrated in Fig. 6. In Fig. 6(a) a spectrum in the high-magnetic-field regime is recorded without prior illumination of the sample with the above-band-gap light of an infrared-light-emitting diode (IR-LED). Therefore no minority electrons are generated, and in this nonequilibrium no electron signal appeared. However, room-temperature black body radiation entering the sample holder via the waveguide is able to ionize the acceptors, thus making possible an accumulation layer in  $p$ -type silicon. The situation can be de-

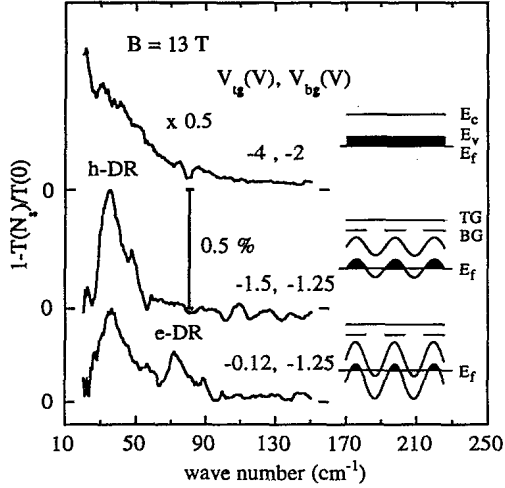


FIG. 5. Transition from an almost 2DHS via a hole dimensional resonance (*h*-DR) to a lateral *n-i-p-i* superlattice (sample B). The insets show schematically the Fermi energy ( $E_f$ ) relative to the spatial modulation of the valence ( $E_v$ ) and conduction-band edges ( $E_c$ ) along the interface.

scribed by two quasi-Fermi levels, one for electrons ( $E_{fe}$ ) and one for holes ( $E_{fh}$ ), with the ones for holes being in equilibrium with the Fermi energy of the back contact. After switching off the IR-LED for charging, thermal equilibrium between the holes and electrons is achieved in adjacent channels and therefore  $E_{fe} = E_{fh}$ . As a consequence the *h*-DR and *e*-DR are observed.

We next want to discuss the transition from a *n-i-p-i* superlattice, in which the electron channels are defined in the gap confinement mode, to a 2DES. For  $V_{tg} = -4$  V and  $V_{bg} = 0$  V, a strong *e*-DR in a quasi-one-dimensional channel can be measured (Fig. 7). On the low-energy side the hole signal appears as a shoulder. The *e*-DR can be

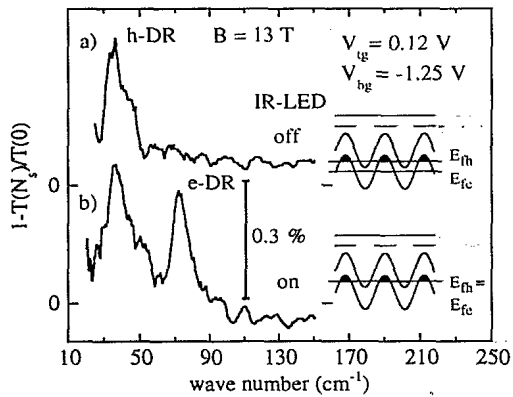


FIG. 6. (a) Formation of holes in a narrow channel under nonequilibrium conditions (IR-LED switched off, sample B). Switching on of the IR-LED shortly before the measurement generates inversion electrons and leads to equilibrium between electrons and holes in neighboring quantum wires (b).  $E_{fe}$  and  $E_{fh}$  refer to the quasi-Fermi levels of electrons and holes. These numbers are identical for the case when the IR-LED is switched on.

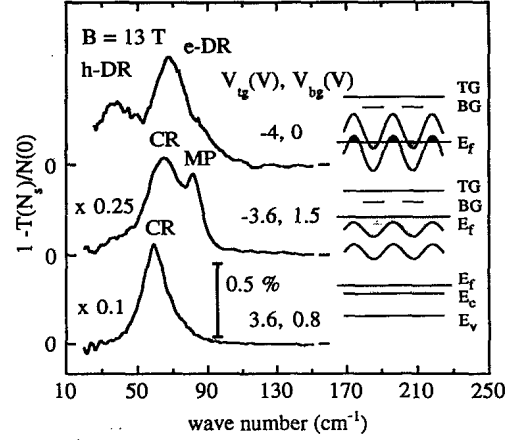


FIG. 7. Spectra (sample B) for the transition from a homogeneous 2DES (CR is the cyclotron resonance) to a density-modulated 2DES (MP is the magnetoplasmon). For  $V_{tg} = -4$  V and  $V_{bg} = 0$  V, a lateral *n-i-p-i* structure is realized. For the explanations of the insets, see Fig. 5.

followed with decreasing magnetic field down to  $B = 0$  T (Fig. 8), and obeys the well-known dispersion<sup>14</sup>  $\omega^2 = \omega_c^2 + \omega_d^2$  ( $\omega_c$  is the cyclotron frequency, and  $\omega_d$  is the frequency of *e*-DR for  $B = 0$  T). For  $V_{tg} = -3.6$  V and  $V_{bg} = 1.5$  V, a weaker density-modulated electron system arises. This can be recognized in the spectrum by the cyclotron resonance (CR) and the magnetoplasmon (MP) at higher energies. The magnetoplasmon energy follows the above-mentioned dispersion law with  $\omega_d$  replaced by  $\omega_p$ .<sup>15</sup> For an almost homogeneous 2DES exclusively, the CR is observed. It can be seen that the cyclotron frequency is shifted for higher electron densities to lower energies.

The magnetic-field dispersion for the characteristic electron excitation in the lateral *n-i-p-i* structure is indicated in Fig. 8. For  $V_{tg} = 0.12$  V and  $V_{bg} = -1.25$  V, the dispersion could only be measured between  $B = 6$  and 15 T. With decreasing magnetic field the position of the *e*-DR shifts much more strongly to lower energies than the *h*-DR. This behavior is expected, since the effective elec-

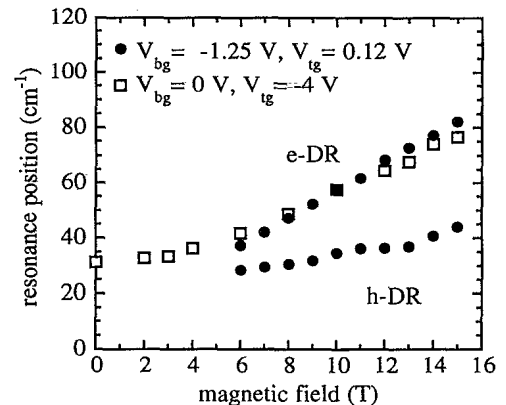


FIG. 8. Magnetic-field dispersion for a lateral *n-i-p-i* superlattice realized by different gate voltages (sample B).

tron mass is much smaller than the effective mass of holes. As shown in earlier experiments<sup>9</sup> the effective mass in a 2DHS is strongly dependent on the hole density, and increases about 50% by changing the carrier density from  $10^{11}$  to  $10^{12}$   $\text{cm}^{-2}$ . Plotting the square of the resonance energy of the holes (Fig. 8) against  $B^2$  gives an effective mass of  $m^* = 0.4m$ . Indeed for very low hole densities a value of  $0.3m$  is expected. It is not well understood so far why the absorption of electrons and holes for  $V_{tg} = 0.12$  V and  $V_{bg} = -1.25$  V has not been observable down to  $B = 0$  T. At low carrier densities, besides the electrostatic confinement of the gate electrodes, the localization of carriers due to a magnetic field or impurities may not become negligible. In high magnetic fields nonlinear screening effects of electrons play an important role.<sup>16</sup> Screening of the external potential transforms a strongly density-modulated electron system at  $B = 0$  T to a system of nonoverlapping electron channels in high magnetic fields.

#### IV. INITIAL INTERBAND STUDIES

In a further step optical transitions between the valence and conduction bands in a lateral *n-i-p-i* superlattice have been investigated. High lateral electric fields in the range of  $10^5$  V/cm predetermine these structures to look for Franz-Keldysh-like effects.<sup>17-19</sup>

Due to the absorption of two metallic gates, the luminescence efficiency was too low so far to observe, besides the phonon-assisted transitions, indications of energy shifts caused by quantization effects. Transmission experiments showed dominantly a strong increase in absorption above the fundamental indirect energy gap  $E_g$  in bulk Si. It is very promising to see that spatially indirect interband transitions in lateral *n-i-p-i* structures have

been measurements of the spectra dependence of the photocurrent. For that, a double-modulation technique has been used. The voltage of the two gates was switched with  $f \sim 1.1$  kHz between nearly flatband case and a lateral *n-i-p-i* potential. Additionally, the incident infrared light was chopped with  $f \sim 16$  Hz. The generated carriers charging and discharging the MOS capacitance result in a photocurrent detected by lock-in amplifiers. This signal as a function of the incident light energy shows a small peak about 60 meV below  $E_g$ . The main advantage of these measurements is that this technique is very sensitive to changes of the electron and hole density at the Si-SiO<sub>2</sub> interface. In contrast to the aforementioned techniques, there is no Si substrate signal. The photocurrent spectra show that in laterally modulated Si structures spatially direct excitonic transitions are dominant. Further experiments in this field are going on.

#### V. CONCLUSIONS

Microstructured lateral periodic gate electrodes on a MOS structure are used in a stacked-gate setup to induce a large lateral potential modulation. FIR experiments are performed on lateral *n-i-p-i* superlattices, and demonstrate that quasi-one-dimensional electron channels alternate with hole channels. The transition from a 2DHS and a 2DES to a lateral *n-i-p-i* structure is studied. At low hole densities a pronounced hole resonance, is observed, and at higher hole densities a Drude-like behavior is seen.

#### ACKNOWLEDGMENT

We would like to thank the Volkswagen Foundation for financial support.

- <sup>1</sup>A. C. Warren, D. A. Antoniadis, and H. I. Smith, *Phys. Rev. Lett.* **56**, 1858 (1986).
- <sup>2</sup>J. H. F. Scott-Thomas, S. B. Field, M. A. Kastner, H. I. Smith, and D. A. Antoniadis, *Phys. Rev. Lett.* **62**, 583 (1989).
- <sup>3</sup>P. F. Bagwell, S. L. Park, A. Yen, D. A. Antoniadis, H. I. Smith, and T. P. Orlando, *Phys. Rev. B* **45**, 9214 (1992).
- <sup>4</sup>J. Alsmeyer, E. Batke, and J. P. Kotthaus, *Phys. Rev. B* **40**, 12 574 (1989).
- <sup>5</sup>I. Jejina, H. Lorenz, J. P. Kotthaus, S. Bakker, and T. M. Klapwijk, *Solid State Commun.* **85**, 601 (1993).
- <sup>6</sup>G. H. Döhler, H. Künzel, D. Olego, K. Ploog, P. Ruden, H. J. Stolz, and G. Abstreiter, *Phys. Rev. Lett.* **47**, 864 (1981).
- <sup>7</sup>A. C. Tselis and J. J. Quinn, *Phys. Rev. B* **29**, 3318 (1984).
- <sup>8</sup>G. Abstreiter, J. P. Kotthaus, J. F. Koch, and G. Dorda, *Phys. Rev. B* **14**, 2480 (1976).
- <sup>9</sup>J. P. Kotthaus and R. Ranvaud, *Phys. Rev. B* **15**, 5758 (1977).
- <sup>10</sup>D. C. Tsui, S. J. Allen, Jr., R. A. Logan, A. Kamgar, and S. N.

Coppersmith, *Surf. Sci.* **73**, 419 (1978).

- <sup>11</sup>W. Hansen, M. Horst, J. P. Kotthaus, U. Merkt, and Ch. Sikorski, *Phys. Rev. Lett.* **58**, 2586 (1987).
- <sup>12</sup>W. Kohn, *Phys. Rev.* **123**, 1242 (1961).
- <sup>13</sup>L. Brey, N. F. Johnson, and B. I. Halperin, *Phys. Rev. B* **40**, 10 647 (1989).
- <sup>14</sup>D. Childers and P. Pincus, *Phys. Rev.* **177**, 1036 (1969).
- <sup>15</sup>T. N. Theis, *Surf. Sci.* **98**, 515 (1980).
- <sup>16</sup>U. Wulf and R. R. Gerhardts, in *Physics and Technology of Submicron Structures*, edited by H. Heinrich, G. Bauer, and F. Kuchar (Springer, Berlin, 1988), p. 162.
- <sup>17</sup>A. Frova and P. Handler, *Phys. Rev. Lett.* **14**, 178 (1965).
- <sup>18</sup>A. Frova, P. Handler, F. A. Germano, and D. E. Aspnes, *Phys. Rev.* **145**, 575 (1966).
- <sup>19</sup>K. I. Britsyn and A. A. Smirnov, *Fiz. Tverd. Tela (Leningrad)* **8**, 163 (1966) [*Sov. Phys. Solid State* **8**, 126 (1966)].